Contents lists available at ScienceDirect

Taiwanese Journal of Obstetrics & Gynecology

journal homepage: www.tjog-online.com

Original Article

Characterization of tubo-ovarian abscess mimicking adnexal masses: Comparison between contrast-enhanced CT, ^{18}F—FDG PET/CT and MRI

Hua Fan [a], Ting-Ting Wang [a], Gang Ren [a], Hong-Liang Fu [b], Xiang-Ru Wu [c], Cai-Ting Chu [a], Wen-Hua Li [a, *]

[a] Department of Radiology, Xinhua Hospital Affiliated to Shanghai Jiao Tong University School of Medicine, 1665 Kong Jiang Road, Shanghai 200092, China
[b] Department of Nuclear Medicine, Xinhua Hospital Affiliated to Shanghai Jiao Tong University School of Medicine, 1665 Kong Jiang Road, Shanghai 200092, China
[c] Department of Pathology, Xinhua Hospital Affiliated to Shanghai Jiao Tong University School of Medicine, 1665 Kong Jiang Road, Shanghai 200092, China

ABSTRACT

Objective: We compared the diagnostic accuracy of contrast-enhanced computed tomography (CT), fluorine 18-labeled—fludeoxyglucose (^{18}F—FDG) positron emission tomography (PET)/CT and conventional magnetic resonance imaging (MRI) without and with diffusion-weighted imaging (DWI) for characterization of tubo-ovarian abscesses (TOAs) that mimic adnexal tumors.
Materials and Methods: We evaluated (retrospectively) 43 patients who underwent contrast-enhanced CT, PET/CT, conventional MRI without and with DWI, and who were found to have TOAs and complex adnexal tumors. All images were evaluated independently by four radiologists using a two-point grading system. Results of contrast-enhanced CT, PET/CT, MRI without DWI, and MRI with DWI were compared for each patient using receiver operating characteristic curves. Sensitivity, specificity, and positive predictive value (PPV) were calculated and compared using the chi-square test.
Results: Sensitivity of MRI with DWI (95%) was significantly higher than that of contrast-enhanced CT (78.6%), PET/CT (86.7%) and MRI without DWI (87.5%). Specificities of these modalities were not significantly different. The PPV of MRI with DWI (100%) was significantly higher than that of the other three modalities (CT, 72.4%; PET/CT 78.5%; MRI without DWI, 81.5%). Overall accuracy of MRI with DWI was significantly higher than that of the other three modalities (CT, 74.4%; PET/CT, 81.4%; MRI without DWI, 83.7%).
Conclusion: MRI with DWI shows high accuracy for characterization of complex ovarian lesions, and is the most useful method for differentiation of TOAs from ovarian tumors.

Introduction

The clinical diagnosis of pelvic inflammatory disease, including tubo-ovarian abscesses (TOAs), is based mainly on the basis of symptoms and signs: pain in the lower abdomen, fever, increased levels of C-reactive protein in blood, and adnexal tenderness. Gastroenterological problems, urinary tract infections, and other gynecologic disease may simulate pelvic inflammatory disease, and some types of chronic pelvic inflammatory disease may mimic malignancy exactly [1—5]. Thus, ascertaining whether a clinically diagnosed complex cystic or cystic-solid mass is inflammatory, benign or malignant is frequently not possible because they include a wide spectrum of inflammatory and neoplastic conditions, ranging from hydrosalpinx to TOAs and from cystadenoma through borderline-to-invasive malignancies. A reliable method to differentiate a benign condition from a malignant condition would provide a basis for optimal preoperative planning, and could reduce the number of unnecessary laparotomies.

Positron emission tomography/computed tomography (PET/CT) combines the anatomic and functional details depicted with CT and metabolic information obtained with PET. Hence, PET/CT yields more precise anatomic information and reduces the number of equivocal PET interpretations. PET/CT and CT have disadvantages, however, such as radiation exposure and limited depiction of small volumes of metabolically active tumors [6—8].

* Corresponding author. 1665 Kongjiang Road, Shanghai, China. Fax: +86 2165795173.
E-mail address: liwenhua@xinhuamed.com.cn (W.-H. Li).

Studies have shown that diffusion-weighted imaging (DWI) can facilitate non-invasive characterization of biologic tissues based on their water-diffusion properties. It yields information about the biophysical properties of tissues: organization and density of cells, microstructure, and microcirculation. Some researchers [9–12] have found that high b-value DWI with measurement of the apparent diffusion coefficient (ADC) is useful in tissue (including serous fluid, mucinous fluid, and pus) and for blood characterization.

Few studies have been conducted comparing contrast-enhanced CT, PET/CT, and magnetic resonance imaging (MRI) with and without DWI for detection of inflammatory and non-inflammatory lesions in the pelvis. Here, we wished to ascertain if addition of a DWI protocol to conventional MRI could be used to help differentiate a pseudo-solid area (pus) from other fluid components.

Methods and methods

Patients

The study protocol was approved by our institutional ethics committee and written informed consent was obtained from all patients. Between January 2008 and May 2016, a DWI sequence was added to conventional MRI for each woman with clinically suspected pelvic inflammatory disease and adnexal masses. We retrospectively analyzed a consecutive population of 336 women who satisfied the following inclusion criteria: (i) history of acute pelvic pain or lower abdominal pain of <3 week duration with or without fever; (ii) lower abdominal tenderness; (iii) bilateral adnexal tenderness and cervical motion tenderness; (iv) increased levels of C-reactive protein (>10 mg/L); (v) increased levels of cancer antigen-125 (>35 UI/L); (vi) available data of contrast-enhanced CT, PET/CT, and MRI with DWI.

The imaging database was reviewed, and subjects who underwent laparoscopy and surgery subsequently were selected. Patients with malignant tumors of the colorectal tract (n = 96) or genitourinary tract (n = 68), endometriomas or hemorrhagic cysts (n = 61), endometrial malignancy (n = 19), hydrosalpinx (n = 16), mature/immature teratomas (n = 15), ovarian fibromas or cystadenofibromas (n = 11), free pelvic fluid only (n = 5), or DWI artifacts (n = 2) were excluded to limit the risk of selection bias [13,14]. Conventional MRI can provide an appropriate diagnosis for endometriomas, mature teratomas, hydrosalpinx, fibromas, cystadenofibromas, and free pelvic fluid, so, these lesions are excluded. The final cohort comprised 43 patients. All these patients were collected and screened by the first author (F.H.).

Image acquisition parameters

CT studies were done using a dual-source 64-channel multidetector CT system (Somatom Definition; Siemens Healthcare, Forchheim, Germany). All patients received 150 mL of 60% iodinated contrast (iohexol (Omnipaque 350); Nycomed Amersham, Little Chalfont, UK) administered via the intravenous route with a power injector at 3 mL/s as well as 800 mL of diatrizoate meglumine (Hypaque, Nycomed Amersham) administered via the oral route. Acquisition of images in the portal venous phase was done with 5–6 mm collimation 60s after injection of contrast material.

In PET/CT examination, all patients fasted for ≥6 h and maintained blood glucose levels <150 mg/dL before PET using ^{18}F–FDG, but oral hydration with glucose-free water was permitted. Patients were allowed to rest in a supine position 40–60 min after injection of ^{18}F–FDG (3 MBq/kg body weight, i.v.). Then, they were positioned for PET/CT. The latter was done on a combined dedicated

PET/CT system (Biograph 64; Siemens Healthcare). A CT image was acquired from the top of the head to mid-thigh without specific instructions for breath-holds. CT parameters were 140 kV, 80 mA, and a slice thickness of 5 mm. CT was followed by PET covering the same transverse field of view during normal breathing. Imaging was acquired with 6–8 bed positions on three-dimensional mode for 3 min per bed position. PET images were reconstructed iteratively using contrast-enhanced CT data for attenuation correction. Co-registered images were displayed on a workstation using dedicated software that allowed viewing of PET, CT and fusion images on trans axial, sagittal and coronal displays.

MRI was done using 3.0-T MR scanners (Signa; GE Medical Systems, Milwaukee, WI, USA) using a torso phased array coil. Axial non-contrast T1-weighted (TR/TE range, 400–600/10–14 ms) and axial T2-weighted (4000–6000/100–120 ms) imaging was done with a chemical shift-selective fat saturation pulse using the following parameters: slice thickness, 6 mm; gap, 1 mm; field of view (FOV), 32–42 cm; matrix, 256 × 256; excitation, 2. Sagittal T1-weighted and T2-weighted (TR/TE range, 3000–6000/100–110 ms) fast spin-echo imaging without chemical shift-selective fat saturation pulses were also under taken, as well as post-contrast enhanced axial and sagittal T1-weighted imaging, using the same parameters as those described above except that a slice thickness of 6 mm was used. DWI-MRI was acquired in the axial plane before administration of contrast medium using a single-shot echo-planar imaging sequence (TR/TE effective range, 8000–10,000/70–100; slice thickness, 6 mm; gap, 1 mm; FOV, 32–42 cm; matrix, 128 × 128; excitation, 2). Also, b values of 0 and 1000 s/mm^2 were applied in three orthogonal (Z, Y, X) directions.

Image analyses

CT data and data for conventional MRI with DWI were reviewed by two radiologists who had 12 years and 13 years of experience in gynecologic imaging. PET/CT images were reviewed by two physicians with expertise in nuclear medicine. Reviewers making assessments of contrast-enhanced CT, MRI and PET/CT were blinded to laparoscopic and pathologic diagnoses of lesions, and assessed all images together in two steps. In the first step, one radiologist measured and recorded the lesion size, standardized uptake value (SUV), and ADC of cystic cavities used for comparison. When the lesion exhibited a multilocular cystic mass, 2–3 regions of interest (ROIs) were drawn within the high signal intensity cystic components, and when the lesion was unilocular, only one ROI was used. The mean size of ROIs varied from 18 to 120 mm^2. To minimize variability, the final ADC value of each patient was determined by the average results of all measured ROIs. In the second step, agreement of the four reviewers was reached after careful evaluation of size, shape, and character (cystic-solid) of the lesion; density of cystic and solid components on CT; signal intensity of cystic and solid components on T1-, T2-, and DWI; PET/CT fusion images by visual inspection. Then, lesions were characterized using a two-point scale: 1 = TOA, 2 = non-TOA (including tumors and ruptured tubal pregnancy).

Statistical analyses

Laparoscopic and surgical pathologic findings were used as reference standards for qualitative assessment of adnexal lesions. Analyses were done using SPSS v17.0 (IBM, Armonk, NY, USA). Quadratic K coefficients were calculated to assess interobserver agreement for contrast-enhanced CT, PET/CT, conventional MRI without DWI, and MRI with DWI with regard to lesion characterization. Rating of "1" suggested a TOA and was accepted as being a

"true positive". Interobserver agreement was based on the k value and agreement: k = 0.00–0.20 is denoted "slight" agreement; 0.21–0.40 = "fair"; 0.41–0.60 = "moderate"; 0.61–0.80 = "substantial"; 0.80–1.00 = "perfect".

Analyses of receiver operating characteristic (ROC) curves were done to compare the diagnostic performance of contrast-enhanced CT, PET/CT, conventional MRI without DWI, and MRI with DWI for each patient. These analyses were followed by comparison of sensitivity and specificity using the McNemar test (two-tailed). The diagnostic accuracy of each reviewer was determined by calculation of the area under the ROC curve (Az) with the chi-square test for each image dataset for the diagnosis of a TOA. Mean ADC values of cystic cavities and SUV were compared using one-way analysis of variance and an unpaired t-test. $p < 0.05$ was considered significant for all analyses.

Results

The final cohort comprised 43 patients (19 pre-menopausal and 24 post-menopausal; mean age, 49.5 (range, 18–79) years). Of these 43 patients, 44.2% (19/43) had a TOA proven by laparoscopic or pathologic means. Twenty-four subjects (55.8%) shown to have non-inflammatory adnexal lesions (6 serous cystadenomas, 4 mucinous cystadenomas, 3 borderline cystadenomas, 7 cystadenocarcinomas, 1 struma ovarii, 2 Krukenberg tumors, and 1 ruptured tubal pregnancy) were selected to serve as control subjects. There is no significant difference of clinical characteristics between the two groups (Table 1).

Findings in all 43 patients revealed considerable variability with regard to contrast-enhanced CT, PET/CT, conventional MRI without DWI, and MRI with DWI, but interobserver agreement was 0.729, 0.793, 0.719 and 0.916, respectively.

ROC analyses showed that the Az of conventional MRI without DWI was lower than that of the image sets (Table 2). Table 3 shows the diagnostic predictive values of adnexal lesions for each method and reviewer. When DWI was added to conventional MRI protocols, the sensitivity, specificity, positive predictive value (PPV), negative predictive value (NPV), and accuracy of MRI findings for prediction of TOAs were 95.0%, 100.0%, 100.0%, 95.8%, and 97.7%, respectively. Thus, a combined DWI strategy may increase the accuracy, sensitivity, and NPV of MRI for distinguishing TOAs from other adnexal masses. Table 4 shows that there was no difference in the mean diameter of lesions, SUV of the solid component, and morphologic characteristics between TOAs and control subjects.

Fluid contents of all cystic cavities of these 43 patients were low density on plain and contrast-enhanced CT. Nevertheless, the signal characteristics of luminal contents of all cystic cavities can demonstrate considerable variability in MRI on T1-weighted and T2-weighted images. Among 19 TOA patients, 36.8% (7/19) had low signal intensity on T1-weighted images and high signal intensity on T2-weighted images, 21.1% (4/19) had intermediate or high signal intensity on T1-weighted images and high signal intensity on T2-weighted images, and 42.1% (8/19) had intermediate or high signal intensity on T1-weighted images and intermediate signal intensity (pseudo-solid or pseudo-soft tissue) on T2-weighted images. All TOAs had high signal intensity on DWI with low ADC ($0.85 \pm 0.31 \times 10^{-3}$ mm^2/s). All luminal contents of cystic components in the control group were low signal intensity on T1-weighted images and high signal intensity on T2-weighted images, and low signal intensity on DWI with high ADC ($2.57 \pm 0.25 \times 10^{-3}$ mm^2/s). TOAs misclassified as adnexal tumors using CT (n = 8), PET/CT (n = 6), and conventional MRI without DWI (n = 5) were all reclassified correctly by taking into account the high signal intensity of luminal contents on DWI with low ADC

Table 2
Comparison of A$_z$ values according to reviewers 1 and 2.

Modality	Reviewer 1	Reviewer 2	p value
CT	0.867 ± 0.05	0.878 ± 0.04	0.09
PET/CT	0.882 ± 0.04	0.896 ± 0.03	0.07
Conventional MRI without DWI	0.855 ± 0.03	0.861 ± 0.05	0.11
Conventional MRI with DWI	0.894 ± 0.02	0.923 ± 0.04	0.06

Table 3
Differential performance between adnexal abscess and adnexal masses.

Parameter	CECT	PET/CT	CMRI	DMRI
No. of TP findings	11	13	14	19
No. of TN findings	21	22	22	23
No. of FP findings	3	2	2	1
No. of FN findings	8	6	5	0
Sensitivity (%)	78.6	86.7	87.5	95.0
Specificity (%)	72.4	78.5	81.5	100.0
PPV (%)	57.9	68.4	73.7	100.0
NPV (%)	87.5	91.7	91.7	95.8
Accuracy (%)	74.4	81.4	83.7	97.7

TP = true positive, TN = true negative, FP = false positive, FN = true negative, PPV = positive predictive value, NPV = negative predictive value, CECT = contrast-enhance CT, CMRI = conventional MRI, DMRI = conventional, MRI with DWI.

Table 4
Characteristics of 43 adnexal lesions on imaging.

Characteristic	Histology		p value
	TOA (n = 19)	non-TOA (n = 24)	
Mean diameter (cm)	4.73	5.19	0.491
SUVmax	9.42	10.79	0.506
Predominantly cystic with unilocular cavity	2/19 (10.5%)	3/24 (12.5%)	0.579
Solid and cystic with multilocularity (≥2)	17/19 (89.5%)	21/24 (87.5%)	0.681
Thickened wall and/or septa (≥3 mm)	15/19 (78.9%)	19/24 (79.2%)	0.587
The ADC value of cystic components	1.06 ± 0.38	2.39 ± 0.32	0.004

Table 1
Clinical characteristics of TOA and non-TOA patients.

Variables	Total (n = 43)	TOA (n = 19)	non-TOA (n = 24)	p value
Age (year)	49.5 ± 18.2 (18–79)	48.2 ± 13.1 (18–77)	51.2 ± 19.6 (20–79)	0.653
Menopausal				
pre	19	9	10	0.801
Post	24	10	14	
Fever				
Yes	22	12	10	0.204
No	21	7	14	
CRP	21.3 ± 9.3 (11.1–40.6)	24.5 ± 8.6 (17.3–40.6)	20.4 ± 7.2 (11.1–38.2)	0.457
CA125	39.2 ± 15.8 (35.1–50.4)	37.6 ± 14.2 (35.1–49.3)	42.5 ± 16.6 (37.2–50.4)	0.525

(Fig. 1). Sometimes it is challenging to make the right diagnosis if there is very little pus in TOA even add the DWI sequence to convention MRI (Fig. 2), and sometimes it is easy to make a differential diagnosis (Fig. 3).

Discussion

We demonstrated that a unilocular or multilocular cystic lesion in the female pelvic cavity is a non-specific finding of an ovarian
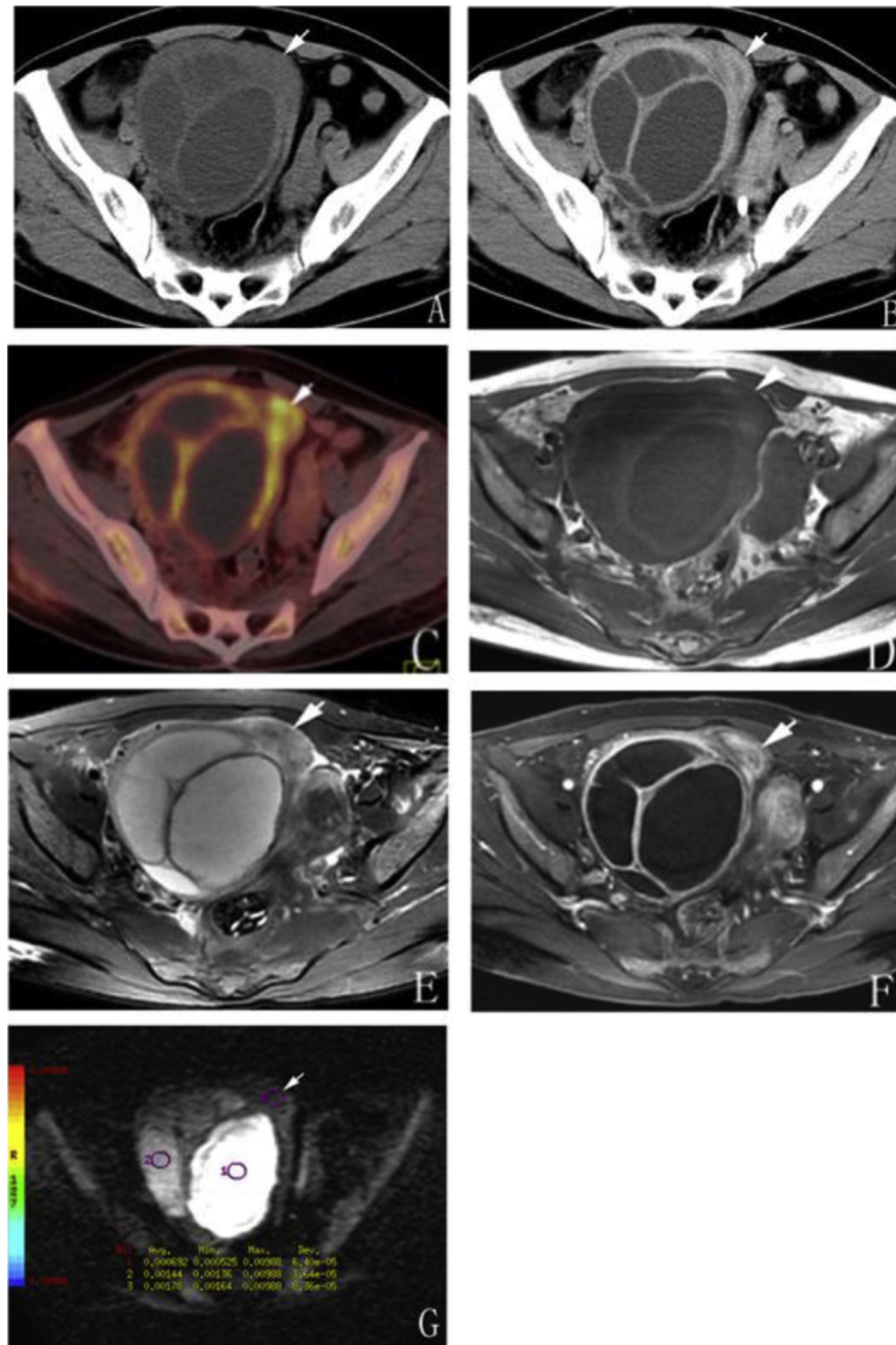
Fig. 1. Ovarian abscess in a 51-year-old woman presenting with abdominal pain. (A) Axial unenhanced CT image shows a well-defined heterogeneous cystic mass with multiple thickened septa and large nodular solid component (arrow). (B) Contrast-enhanced CT scan reveals that the mass is enhanced predominantly with thickened wall, septa and a nodular solid component (arrow). (C) Fusion PET/CT image shows high uptake of 18F—FDG along the wall-thickened area and solid component with a SUVmax of 12.4 (arrow) (D) Axial T1-weighted image shows a mass with an iso and mildly low mixed signal intensity in the pelvic cavity. (E) Axial T2-weighted image reveals that the mass is heterogeneous high signal intensity and the solid component is slightly hyperintensity (arrow). (F) Axial contrast-enhanced MRI shows a complex cystic and solid mass with strikingly enhanced walls, septa and solid component (arrow). The figure (A), (B), (C), (D), (E) and (F) suggested an ovarian tumor diagnosis of the lesion, but on figure (G), Axial DWI, shows multiple, ovoid, high-signal-intensity areas, findings that are compatible with an ovarian abscess.
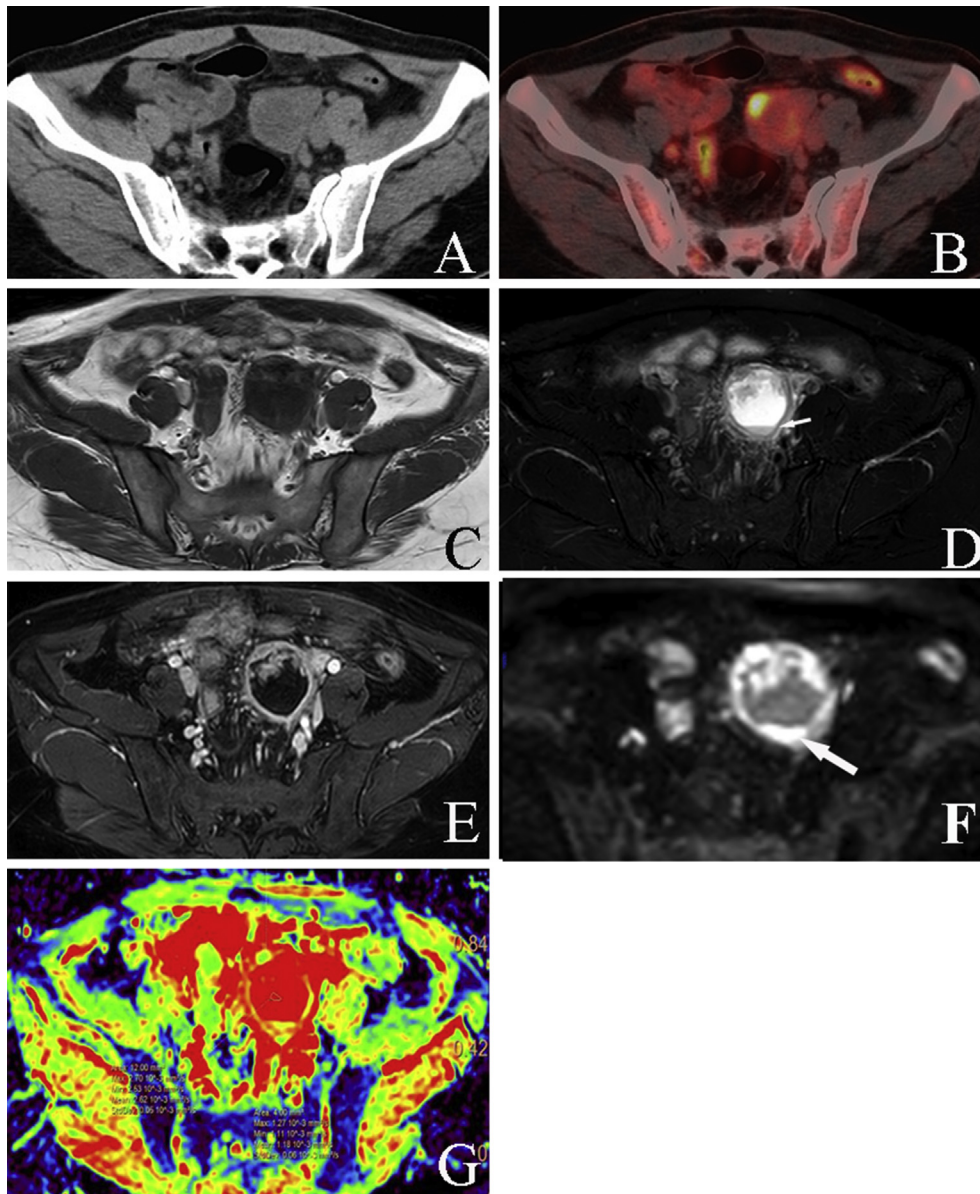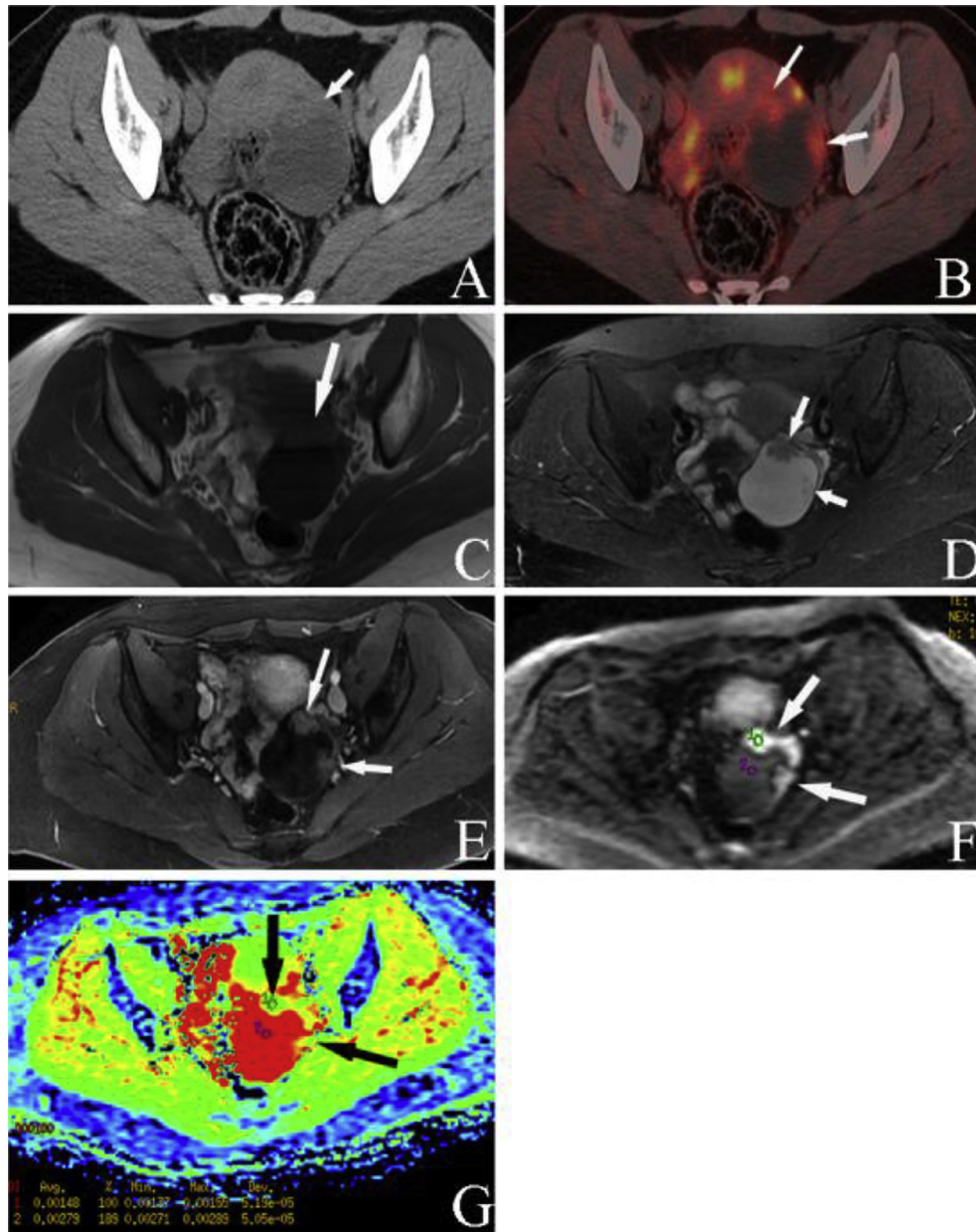
Fig. 2. TOA in a 35-year-old woman presenting with dull lower abdominal pain for 2 weeks. (A) Axial non-contrast-enhanced CT image demonstrates an oval mass in left adnexal area, in front which is the slightly high density nodular solid component. (B) Fusion PET/CT image shows high uptake of ^{18}F–FDG of solid component with a SUVmax of 8.3. (C) The axial T1WI shows that mass mixes scattered iso-hyper signal intensity floccules into low signal intensity part. (D) The axial T2WI reveals that the mass is heterogeneous, the solid component is slightly hyperintensity (arrow), mention that there is a small fluid–fluid level in the back of the mass with hyper and slightly hyper signal intensity on either side (arrow). (E) Showed that the solid components is strikingly enhanced. (F) and (G) On DWI and ADC map, the bulk of the cystic component is lower signal with high ADC value. There are small high signal intensity part in the back of the mass on DWI, in combination with its slightly hyper signal intensity on T2WI, we can draw the diagnosis of TOA.

tumor, and that various inflammatory and neoplastic processes (ranging from cystadenoma through borderline to invasive malignancy, and from hydrosalpinx to TOAs) can have a similar appearance. Moreover, accurate evaluation of adnexal lesions is important for optimal treatment planning. Our results demonstrate that DWI in combination with conventional MRI is sensitive and specific for establishing the diagnosis of a TOA, and for distinguishing a TOA from other pathologic processes. With the use of ADC measurements and signal characteristics, MRI with DWI can lead to correct assessment of a TOA with a high degree of accuracy.

DWI has been used to improve conventional MRI by allowing identification of specific diagnostic criteria according to the tissue specificities of tumors in the brain, breast, prostate gland, and abdomen [15–21]. However, until now, no such data have been

available for patients with TOAs. The latter may produce very complex masses with wall thickening and pseudo-solid areas. Such areas can demonstrate low, intermediate, or high signal intensity on T1-weighted images and low or intermediate signal intensity on T2-weighted images, and are similar to those of soft-tissue or mucinous components of adnexal masses. The signal characteristics of pseudo-solid areas may be related to the presence of: (i) many inflammatory cells, a matrix of proteins, cellular debris, and bacteria in high-viscosity purulent fluids; (ii) large molecules restricting proton diffusion. Hence, pseudo-solid areas can demonstrate marked enhancement, thereby mimicking malignancy.

The clinical features of acute infection and malignancy in the pelvis usually differ, though some chronic infections (e.g., TOAs) may mimic malignancy exactly [4,22,23]. In our patients, initially all TOA cavities had high signal intensity on DWI with low ADC. Hence,

Fig. 3. Serous borderline cystadenoma in a 26-year-old woman who presented with dull lower abdominal pain and a finding of left adnexal mass for 7 months. (A) Axial non-contrast-enhanced CT image demonstrates an oval mass in left adnexal area, in front which is the moderately high density nodular solid component (arrow). (B) Fusion PET/CT image shows high uptake of ^{18}F–FDG of solid component with a SUVmax of 4.2 (arrow). (C) and (D) The cystic component of the mass is long T1, long T2 material and solid component is iso signal intensity both on T1 and T2 image (arrow). (E) Axial contrast-enhanced T1WI shows a complex cystic and solid mass with strikingly enhanced walls and solid component (arrow). (F) and (G) The low signal intensity of cystic component on DWI and a high ADC value on ADC map can exclude the diagnosis of TOA.

addition of DWI enabled us to increase the diagnostic confidence of conventional MRI in ≤22.5% of TOAs and ovarian abscesses. This positive result was mainly because addition of DWI to conventional MRI can be used to differentiate (with considerable confidence) pseudo-solids from other conditions based on signal characteristics. If high signal intensity area is depicted on DWI with low ADC, our results demonstrate that high or intermediate signal intensity on T2-weighted images of this area without enhancement are the best criteria for TOA prediction. These findings are similar to our previous report that demonstrated a relationship between high signal intensity with low ADC [2].

CT is used worldwide in the staging and follow-up of malignant tumors in the pelvis because of its fast throughput of examinations, high image quality, and lower cost than PET/CT and MRI. However, its usefulness in differentiating ovarian processes is limited because

soft-tissue contrast is relatively poor compared with that using MRI, so CT has lower diagnostic accuracy [24,25]. The sensitivity (57.9%), specificity (87.5%), PPV (78.6%), NPV (72.4%), and accuracy (74.4%) of CT for TOA detection in our study were lower than that of PET/CT and MRI without or with DWI. These findings could have been caused by two factors: (i) the TOA may produce very complex masses with a thickened/irregularly contrasted wall and pseudo-solid areas because of inflammatory exudation; (ii) the TOA cavity and cystic components have similar low densities on CT. These conditions are enhanced considerably and can mimic malignancy exactly.

PET/CT enables acquisition of metabolic data and anatomic data, and provides precise anatomic localization of suspicious areas of high uptake of ^{18}F–FDG. PET/CT is an accurate modality for assessment of primary and recurrent ovarian tumors if

conventional imaging (e.g., ultrasound, CT, MRI) is inconclusive or negative. The sensitivity and diagnostic accuracy of PET/CT in characterization of TOAs was 73.7% and 83.7%, respectively, in our study. This low sensitivity and low accuracy may have been because TAO walls with inflammatory exudation could result in increased uptake of ^{18}F—FDG, and led to misclassification as adnexal tumors [26,27]. The SUVmax, which was not significantly different in the two groups, may have been another reason for such low sensitivity and low accuracy. Several studies have shown that many false-positive PET/CT findings for detection of primary lesions and nodal metastasis in the chest, head and neck can be attributed instead to inflammation [27,28].

The present study had three main limitations. First, all patients were selected carefully and the number of patients who underwent CT, PET/CT and MRI was relatively small. Second, the signal intensity and ADC of pus are affected by: protein concentrations; number of inflammatory cells and bacteria with different pathogenic organisms; age of the abscess; fluid viscosity. Hence, some of the conclusions drawn from our results may not be applicable generally. Finally, none of our patients underwent dynamic contrast-enhanced CT and MRI. According to a previously established classification of time—signal intensity curves, the pattern of dynamic enhancement can help to distinguish between benign, borderline, and invasive ovarian tumors.

We demonstrated that DWI in combination with conventional MRI is useful for improving the characterization of clinically suspected pelvic inflammatory diseases. With the use of ADC measurements and signal characteristics, MRI can lead to a more accurate assessment of adnexal lesions.

Conflicts of interest

The authors have no conflicts of interest relevant to this article.

Acknowledgements

References

[1] Thomassin-Naggara I, Toussaint I, Perrot N, Rouzier R, Cuenod CA, Bazot M, et al. Characterization of complex adnexal masses: value of adding perfusion- and diffusion-weighted MR imaging to conventional MR imaging. Radiology 2011;258:793—803.

[2] Li WH, Zhang YZ, Cui YF, Zhang P, Wu XR. Pelvic inflammatory disease: evaluation of diagnostic accuracy with conventional MR with added diffusion-weighted imaging. Abdom Imag 2013;38:193—200.

[3] Sohaib SAA, Sahdev A, Trappen PV, Jacobs IJ, Reznek RH. Characterization of adnexal mass lesions on MR imaging. AJR 2003;180:1297—304.

[4] Foti PV, Ognibene N, Spadola S, Caltabiano R, Farina R, Palmucci S, et al. Non-neoplastic diseases of the fallopian tube: MR imaging with emphasis on diffusion-weighted imaging. Insights Imag 2016;7(3):311—27.

[5] Medeiros LR, Freitas LB, Rosa DD, Silva FR, Silva LS, Birtencourt LT, et al. Accuracy of magnetic resonance imaging in ovarian tumor: a systematic quantitative review. Am J Obstet Gynecol 2011;204:67.e1-10.

[6] Kim C, Chung HH, Oh SW, Kang KW, Chung JK, Lee DS. Differential diagnosis of borderline ovarian tumors from stage I malignant ovarian tumors using FDG/CT. Nucl Med Mol Imaging 2013;47:81—8.

[7] Beiderwellen K, Grueneisen J, Ruhlmann V, Buderath P, Aktas B, Heusch P, et al. [(18)F]FDG PET/MRI vs. PET/CT for whole-body staging in patients with recurrent malignancies of the female pelvis: initial results. Eur J Nucl Med Mol Imaging 2015;42:56—65.

[8] Queiroz MA, Kubik-Huch RA, Hauser N, Freiwald-Chilla B, von Schulthess G, Froehlich JM, et al. PET/MRI and PET/CT in advanced gynaecological tumours: initial experience and comparison. Eur Radiol 2015;25:2222—30.

[9] Bakir B, Bakan S, Tunaci M, Bakir VL, Iyibozkurt AC, Berkman S, et al. Diffusion-weighted imaging of solid or predominantly solid gynaecological adnexal masses: is it useful in the differential diagnosis? Br J Radiol 2011;84:600—11.

[10] Bollineni VR, Kramer G, Liu Y, Melidis C, deSouza NM. A literature review of the association between diffusion-weighted MRI derived apparent diffusion coefficient and tumour aggressiveness in pelvic cancer. Cancer Treat Rev 2015;41:496—502.

[11] Malek M, Pourashraf M, Mousavi AS, Rahmani M, Ahmadinejad N, Alipour A, et al. Differentiation of benign from malignant adnexal masses by functional 3 tesla MRI techniques: diffusion-weighted imaging and time-intensity curves of dynamic contrast-enhanced MRI. Asian Pac J Cancer Prev 2015;16: 3407—12.

[12] Mukuda N, Fujii S, Inoue C, Fukunaga T, Tanabe Y, Itamochi H, et al. Apparent diffusion coefficient (ADC) measurement in ovarian tumor: effect of region-of-interest methods on ADC values and diagnostic ability. J Magn Reson Imag 2016;43:720—5.

[13] Thawait SK, Batra K, Johnson SI, Torigian DA, Chhabra A, Zaheer A. Magnetic resonance imaging evaluation of non ovarian adnexal lesions. Clin Imag 2016;40(1):33—45.

[14] Anthoulakis C, Nikoloudis N. Pelvic MRI as the "gold standard" in the subsequent evaluation of ultrasound-indeterminate adnexal lesions: a systematic review. Gynecol Oncol 2014;132(3):661—8.

[15] Winter LM, Sommer G, Bongartz G. High-field magnetic resonance imaging of the pelvis: uterus, ovary, and prostate gland. Top Magn Reson Imag 2010;21: 177—88.

[16] Li HM, Qiang JW, Xia GL, Zhao SH, Ma FH, Cai SQ, et al. Primary ovarian endometrioid adenocarcinoma: magnetic resonance imaging findings including a preliminary observation on diffusion-weighted imaging. J Comput Assist Tomogr 2015;39(3):401—5.

[17] Cappabianca S, Iaselli F, Reginelli A, DAndrea A, Urraro F, Grassi R, et al. Value of diffusion-weighted magnetic resonance imaging in the characterization of complex adnexal masses. Tumori 2013;99(2):210—7.

[18] Oh JW, Rha SE, Oh SN, Park MY, Byun JY, Lee A. Diffusion-weighted MRI of epithelial ovarian cancers: correlation of apparent coefficient values with histologic grade and surgical stage. Eur J Radiol 2015;84:590—5.

[19] Li WH, Chu CT, Cui YF, Zhang P, Zhu MJ. Diffusion-weighted MRI: a useful technique to discriminate benign versus malignant ovarian surface epithelial tumors with solid and cystic components. Abdom Imag 2012;37:897—903.

[20] Winfield JM, deSouza NM, Priest AN, Wakefield JC, Hodgkin C, Freeman S, et al. Modelling DW-MRI data from primary and metastatic ovarian tumours. Eur Radiol 2015;25(7):2033—40.

[21] Mimura R, Kato F, Tha KK, Kudo K, Konno Y, Oyama-Manabe N, et al. Comparison between borderline ovarian tumors and carcinomas using semi-automated histogram analysis of diffusion-weighted imaging: focusing on solid components. Jpn J Radiol 2016;34:229—37.

[22] Ueda H, Togashi K, Kataoka ML, Koyama T, Fujiwara T, Fujii S, et al. Adnexal masses caused by pelvic inflammatory disease: MR appearance. Magn Reson Med Sci 2002;15(1):207—15.

[23] Tsuboyama T, Tatsumi M, Onishi H, Nakamoto A, Kim T, Hori M, et al. Assessment of combination of contrast-enhanced magnetic resonance imaging and positron emission tomography/computed tomography for evaluation of ovarian masses. Invest Radiol 2014;49:524—31.

[24] Ratner ES, Staib LH, Cross SN, Raji R, Schwartz PE, McCarthy SM. The clinical impact of gynecologic MRI. AJR Am J Roentgenol 2015;204:674—80.

[25] Thomassin-Naggara I, Bazot M. MRI and CT-scan in presumed benign ovarian tumors. J Gynecol Obstet Biol Reprod 2013;42:744—51.

[26] Kim YI, Kim SK, Lee JW, Lee SM, Kim TS. Ovarian mass mimicking malignancy: a case report. Nucl Med Mol Imaging 2010;44:290—3.

[27] Rakheja R, Makis W, Hickeson M. Bilateral tubo-ovarian abscess mimicks ovarian cancer on MRI and 18F-FDG PET/CT. Nucl Med Mol Imaging 2011;45: 223—8.

[28] Kim CK, Chung HH, Oh SW, Kang KW, Chung JK, Lee DS. Differential diagnosis of borderline ovarian tumors from stage I malignant ovarian tumors using FDG PET/CT. Nucl Med Mol Imaging 2013;47:81—8.